

# MICROSTRUCTURE OF TITANIUM ALLOYS PRODUCED BY THE METHOD OF LAYER-BY-LAYER ELECTRON BEAM SURFACING USING THE WIRE OF GRADE Ti6Al4V

V.M. Nesterenkov, M.O. Rusnyk, O.M. Berdnikova, V.A. Matviichuk and V.R. Strashko

E.O. Paton Electric Welding Institute of the NAS of Ukraine

11 Kazymyr Malevych Str., 03150, Kyiv, Ukraine. E-mail: [office@paton.kiev.ua](mailto:office@paton.kiev.ua)

The specimens of products of titanium alloy of various shapes using the wire of grade Ti6Al4V were produced by electron beam surfacing. In the deposited layers no defects were detected. In the course of the work, the investigations of microstructure, phase composition and mechanical properties of the specimens were carried out. For the deposited metal, the structure consisting mainly of lamellar-acicular  $\alpha'$ -phase is typical. The structure contains a small amount of  $\beta$ -phase, which lies in the form of thin interlayers layers between the acicular precipitations of  $\alpha'$ -phase. It is not detected using the optical microscope, however can be detected applying electron microscopy and X-ray examinations. The microstructure of the deposited metal is mostly equilibrium and granular, gradient in sizes and microhardness. The microhardness of the boundary zones differs from the microhardness of the grain matrix, which may be associated with the difference in the content of alloying elements. Towards the top of the built specimen, the hardness decreases slightly. 9 Ref., 1 Table, 9 Figures.

*Keywords:* additive technologies, electron beam gun, electron beam surfacing, titanium alloy, metallography, microstructure, microhardness

Today, additive technologies is one of the promising areas that are rapidly developing in industrial production. The market of additive technologies consists of production of the equipment and its maintenance, development of the software, models of the future parts and creation of products according to drawings of the customer.

The additive equipment includes many software and hardware machines that perform various tasks and functions. Among them, manufacture of products according to the digital model applying the method of layer-by-layer deposition of consumables remains common [1].

Laser additive technologies have become the most widespread. However, to create large, material-intensive products like housings, an increased efficiency of layer-by-layer surfacing is required. In this case, it is most advantageous to use the energy of the electron beam, which is focused and supplied directly into the zone of alloy by the electron-optical system of the electron beam gun (EBG).

The use of electron beam additive technologies in aircraft and turbine construction, where light, chemically active materials based on aluminum and titanium are used, is especially relevant. The process takes place in vacuum, which allows surfacing a part without additional shielding gases, at the same time maintaining the purity of the original material.

In this work, the studied material was titanium Ti6Al4V alloy, produced by electron beam surfacing.

Titanium alloys are one of the main structural materials currently applied in various industries. Among titanium alloys Ti6Al4V is widespread. It is widely used in aerospace and medical fields. Namely in these industries the task of rapid and simple creation of a wide range of nomenclature products [2, 3] from Ti6Al4V alloy is set.

The aim of the work was to study microstructures and microhardness of specimens from Ti6Al4V alloy made by layer-by-layer growing using electron beam additive technology by filler wire.

To achieve this aim, the following tasks were set in the work:

- holding the specimens welded in vacuum by the wire of grade Ti6Al4V;
- study of microstructure of the deposited specimens;
- measurement of microhardness of specimens.

**Electron beam surfacing using wire.** The surfacing technology consists in layer-by-layer deposition of metal in the form of a wire, which is melted by electron beam gun to produce a workpiece, the geometry of which is as close to the final product as possible. The advantage of the technology is a high speed of product manufacturing, which is up to 12 kg/h. The technology allows manufacturing large-sized metal products, including those of refractory and heat-resistant alloys with a high density and homogeneity [4].

V.M. Nesterenkov — <http://orcid.org/0000-0002-7973-1986>, M.O. Rusnyk — <https://orcid.org/0000-0002-7591-7169>,  
O.M. Berdnikova — <http://orcid.org/0000-0001-9754-9478>, V.A. Matviichuk — <https://orcid.org/0000-0002-9304-6862>,  
V.R. Strashko — <https://orcid.org/0000-0001-6852-3551>

© V.M. Nesterenkov, M.O. Rusnyk, O.M. Berdnikova, V.A. Matviichuk and V.R. Strashko, 2020

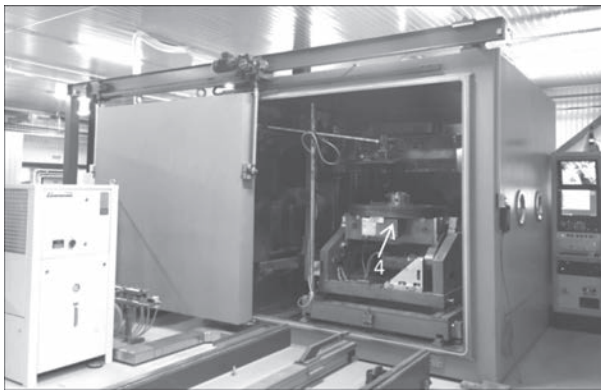


**Figure 1.** Electron-beam installation with mechanism for moving and feeding wire for surfacing

A high repeatability of the results of electron beam surfacing technology in combination with the flexibility of the process control allows forming parts with the required structure and specified properties. During the surfacing process, the electron beam creates a pool of the molten metal on the surface of a part. The part being deposited moves relative to the fixed electron gun and the filler wire feed mechanism, or the electron gun with the wire feed device moves relative to the fixed base [5, 6].

To manufacture product specimens, a wire with the diameter of 2 mm of grade Ti6Al4V was used. Surfacing was carried out in the electron beam installation equipped with the mechanism for moving and feeding wire (Figures 1, 2).

For investigations linear and cylindrical specimens were deposited.

The process of electron beam surfacing takes place in vacuum chamber (Figure 1). The wire is fed from the coil by electric motor with reducer through the guide channel 1 and the nozzle 2 to the surfacing zone (Figure 2). In the process of surfacing, the variable parameters are wire feed rate and beam current. The surfacing is layer-by-layer, after each pass the manipulator is risen to a set value in the coordinate  $Z$ - $Z$ . The cylindrical specimen was produced by rotating the surface to be deposited 3 by means of the vertical rotator 4 (Figure 2, *a*) relative to the fixed EBG 5. The linear specimen was

Chemical composition of the wire Ti6Al4V, wt.%

V	Al	Fe	N	O	H	C
3.5–4.5	5.5–6.75	0.4	0.05	0.2	≤0.015	0.08

produced by moving EBG 5 with the wire feed manipulator relative to a rigidly fixed plate 6.

Thus, the following specimens were produced: cylindrical – with a diameter of 70 mm, 30 mm height and a wall thickness of 9–10 mm. And a linear one of 100 mm length, 40 mm height with a wall thickness of 7.8 mm.

The chemical composition of the wire of Ti6Al4V alloy is given in the Table.

**Metallographic examinations.** To reveal microstructure, the polished sections of deposited specimens were etched in a special reagent for etching titanium and its alloys of the following composition:

- hydrofluoric acid — 1 part;
- nitric acid — 1 part;
- water — 1 part.

Metallographic examinations were carried out in the microscope «Neophot-32» at different magnifications. The digital images of microstructures were obtained with the help of the «Olympus» camera. The Vickers hardness of the examined metal was measured in the microhardness tester M-400 of the Company LECO at the loads of 1.0 kg ( $HV_{10}$ ) throughout the entire height of the sections with a step of 500  $\mu\text{m}$  and 0.1 kg ( $HV_1$ ) for detailed examinations of the structure.

**Cylindrical specimen.** The specimen consists of 14 layers of deposited metal (Figure 2). Metallographic examinations of the deposited metal show that the structure mainly consists of recrystallized grains of different sizes with different degrees of etching. In the areas of the deposited metal no microdefects were detected.

In the lower part of the specimen (Figure 3, layers 1–4) the grain structure is mainly uniform, but as to the grain size the structure is gradient:  $D_g$  (min) = 500–700  $\mu\text{m}$ ;  $D_g$  (max) = 1800–2000  $\mu\text{m}$ . Figure 4, *a* shows the change of the minimum and maximum grain sizes ( $D_g$ ) and the length of the crystallites ( $L_{cr}$ ) throughout the height of the specimen in the deposited layers.

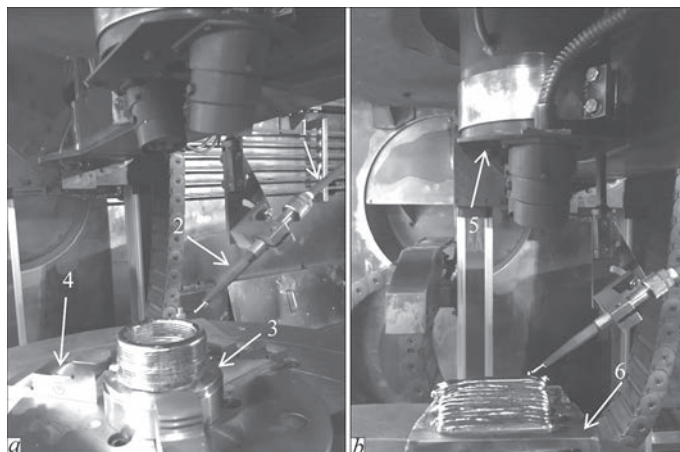


**Figure 2.** Specimens deposited by electron beam: *a* — cylindrical; *b* — linear

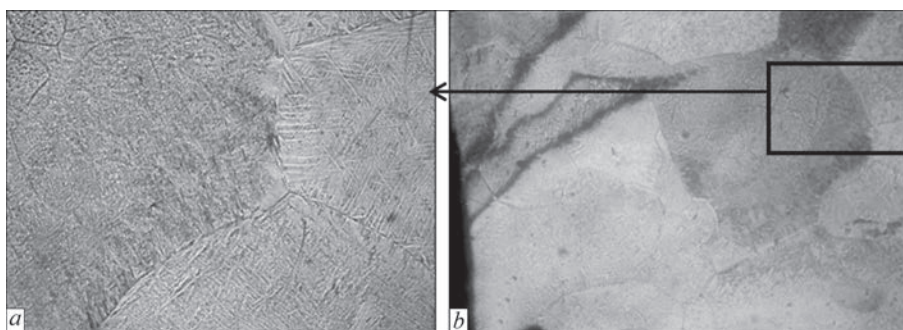


**Figure 3.** Microstructure of metal in the lower zone of the specimen: *a, b* – fragments of microstructure: *a* —  $\times 100$ ; *b* —  $\times 25$

**The hardness distribution is nonuniform.** The values of hardness ( $HV_{10}$ ) and its change throughout the entire height of the cylindrical specimen are graphically shown in Figure 4, *b*.

During the transition to the next layers, the formation of large crystallites throughout the entire height of the specimen and a slight decrease in hardness with its relatively uniform distribution and characteristic values of  $HV_{10}$ –2750–2820 MPa are observed (Figure 4, *b*). It is established that in the recrystallized areas of the deposited metal the hardness is in the range from  $HV_{10}$ –2600 to  $HV_{10}$ –3130 MPa (Figure 5). In a more detailed examination of the structure (at a magnification of  $\times 100$ ) the following was established. For the deposited metal, the structure is characteristic, consisting mainly of a lamellar-acicular  $\alpha'$ -phase (Figures 5, 6).

In the boundary zones of  $\alpha'$ -phase, the etchability of which is weaker than the grain matrix, the hardness amounts to  $HV_{10}$ –2870–3660 MPa. The microhardness of the boundary zones differs from the microhardness of the grain matrix, which may be associated with the difference in the composition of the alloying elements [4].

According to [7], the structure obviously contains a small amount of  $\beta$ -phase, which lies in the form of thin interlayers between the acicular precipitations of  $\alpha'$ -phase and is not detected by optical microscope, but is determined by electron microscopy and X-ray examinations.

In deposition of the surfacing layers, as a result of heat treatment, throughout the height of the specimen, the structure represents large crystallites with a homogeneous lamellar-acicular structure of  $\alpha'$ -phase at the microhardness  $HV_{10}$ –2830–3220 MPa. The sizes and

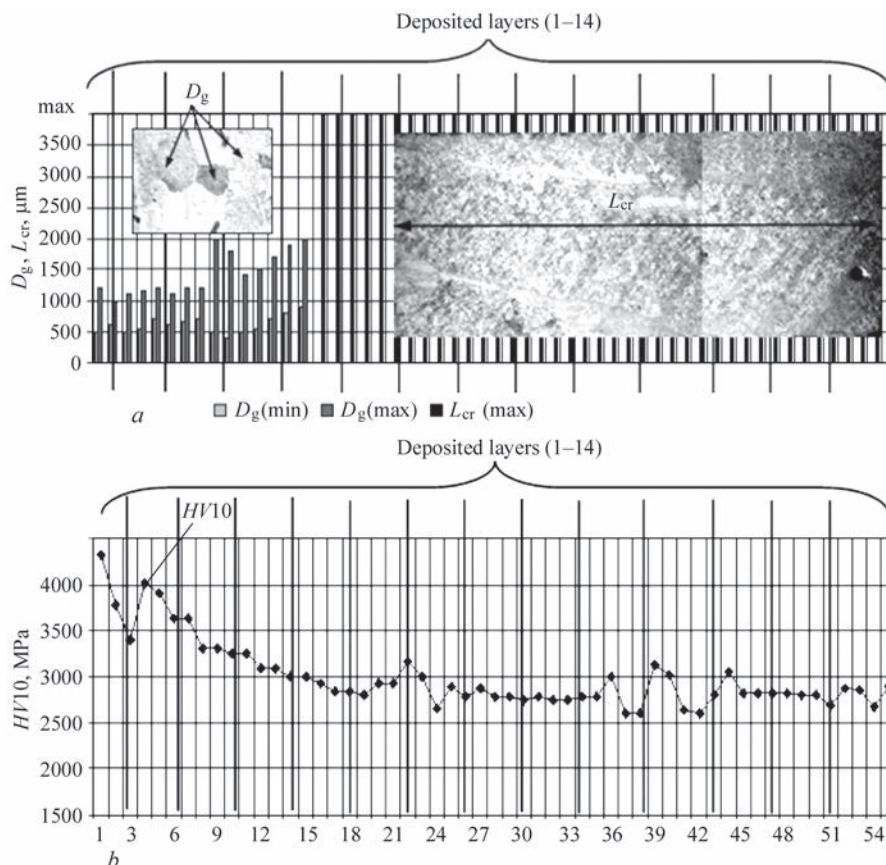


**Figure 4.** Change of structural parameters in the deposited layers: *a* — grain size ( $D_g$ ); *b* — microhardness ( $HV_{10}$ )

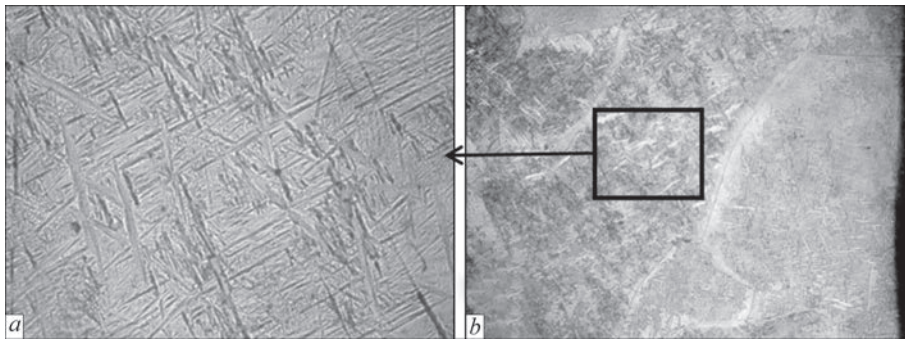


**Figure 5.** Microstructure of metal in the middle part of the specimen: *a, b* — fragments of microstructure: *a* —  $\times 100$ ; *b* —  $\times 25$

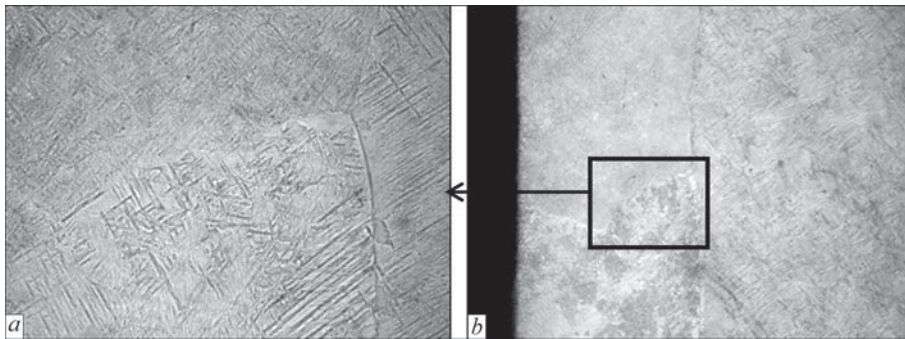


**Figure 6.** Microstructure of metal in the upper zone of the specimen: *a, b* — fragments of microstructure: *a* —  $\times 100$ ; *b* —  $\times 25$

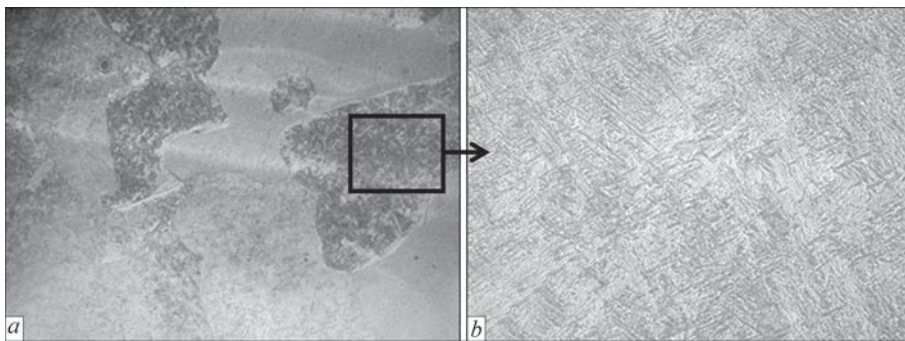


**Figure 7.** Microstructure of metal in the lower zone of the linear specimen: *a, b* — fragments of microstructure: *a* —  $\times 25$ ; *b* —  $\times 200$

a shape of needles and plates depend on the purity and cooling rate of the metal [8]. The middle layer of the deposited metal is characterized by a thickening of the acicular component of  $\alpha'$ -phase (Figure 5). It is known that with decreasing cooling rate the acicular precipitations of  $\alpha'$ -phase are thickened [7].

**Linear specimen.** Surfacing consists of 12 layers (Figure 2, *b*). No structural defects were detected.

Metallographic examinations of the deposited metal showed that as well as in the cylindrical specimen, the structure consists of recrystallized grains of different sizes with different degrees of etchability.

In the lower part of the specimen (Figure 7, layers 1–8) the grain structure has a mixed character: relatively equilibrium grains and grains of irregular shape.

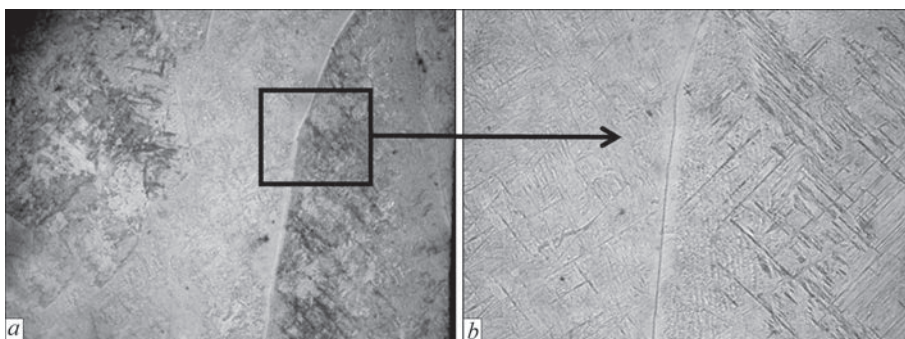


**Figure 8.** Microstructure of metal of the linear specimen in the upper zone: *a, b* — fragments of microstructure: *a* —  $\times 25$ ; *b* —  $\times 100$

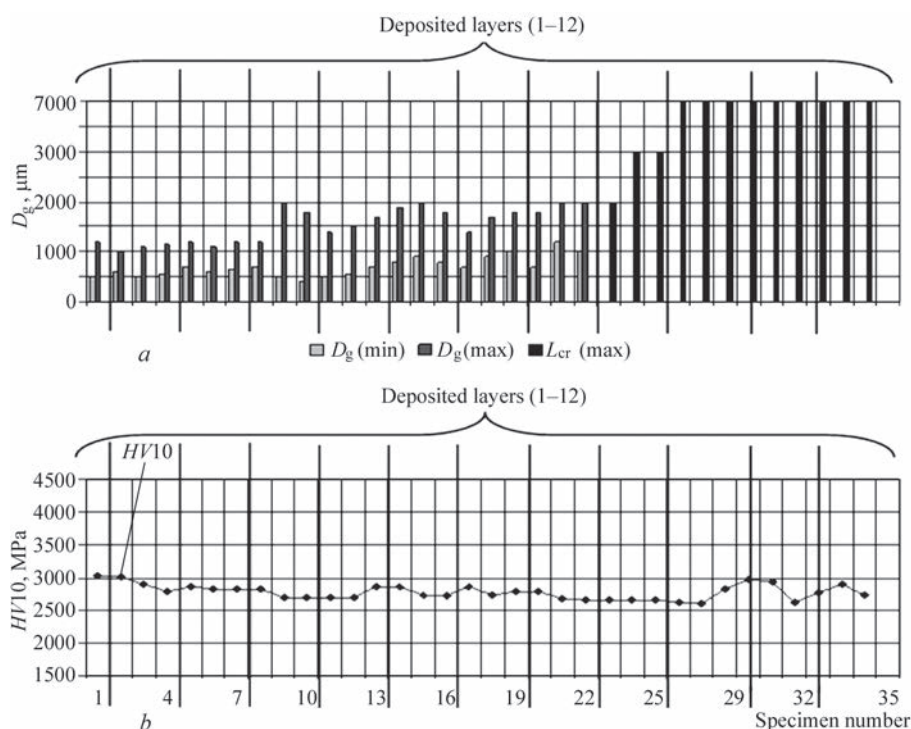


**Figure 9.** Change of structural parameters in the deposited layers: *a* — grain size ( $D_g$ ); *b* — microhardness ( $HV_{10}$ )

The grain size ( $D_g$ ) in this zone is about  $D_g = 500\text{--}1600 \times 700\text{--}4000 \mu\text{m}$ . The distribution of microhardness is relatively uniform. During the transition to the next layers (9–12), the formation of large crystallites of the size up to  $h \times L_{cr} = 2000 \times 7000 \mu\text{m}$  is observed (Figures 8, 9, *a*).

The values of hardness ( $HV_{10}$ ) and its change throughout the entire height of the linear specimen are shown in (Figure 9, *b*). In the lower layer  $HV_{10}$ –3030 MPa. At the transition to the next layers the hardness slightly decreases to  $HV_{10}$ –2790–3010 MPa. It was established that the hardness throughout the entire height of the deposited metal is in the range from  $HV_{10}$ –2630 to  $HV_{10}$ –2930 MPa.

During a detailed examination of the deposited metal (magnification  $\times 100$ ) it was found that the structure consists of a lamellar-acicular  $\alpha'$ -phase (Figures 7, 8). The microhardness in the inner volumes of the grain structure is  $HV_{10}$ –2210–2970 MPa. In the boundary zones of grains there are no areas with a low etchability. Their structure is the same as the grain matrix. This indicates the absence of chemical heterogeneity in the local areas of the structural components [7].

## Conclusions

1. The applied technology of multilayer surfacing allows producing structure of cast metal without defects in the deposited layers.

2. Investigations of the structure of multilayer surfacing showed that in the lower layers mostly equilibrium grain structure is formed, gradient in sizes and microhardness ( $HV_{10}$ ).

3. Massive crystallites are formed throughout the entire height of the investigated specimens (except for the lower layers). The inner lamellar-acicular structure of  $\alpha'$ -phase grains is homogeneous and larger than in the lower layers.

- Iliin, A.A., Kolachev, B.A., Polkin, I.S. (2009) *Titanium alloys. Composition, structure, properties*: Manual. Moscow, VILS-MATI [in Russian].
- Al-Bermani, S.S., Blackmore, M.L., Zhang, W, Todd, I. (2010) The origin of microstructural diversity, texture, and mechanical properties in electron beam melted Ti–6Al–4V. *Metallurg. and Mater. Transact. A*, 41(13), 3422–3434. doi:10.1007/s11661-010-0397-x
- Popov, A.A., Illarionov, A.G., Rossina, N.G., Grib, S.V. (2013) *Physical metallurgy and heat treatment of titanium alloys. Structure and properties*: Manual. Ekaterinburg, UrFU [in Russian].
- Zhukov, V.V., Grigorenko, G.M., Shapovalov, V.A. (2016) Additive manufacturing of metal products (Review). *The Paton Welding J.*, 5–6, 137–142.
- Matviichuk, V.A., Nesterenkov, V.M., Rusynik, M.O. (2018) Application of additive electron-beam technologies for manufacture of metal products. *Electrotechnica & Electronica E+E*, 3–4, 69–73.
- Nesterenkov, V.M., Matviichuk, V.A., Rusynik, M.O. (2017) Principles of production of commercial items by rapid prototyping using electron beam technologies. In: *Proc. of 8<sup>th</sup> Int. Conf. on Beam Technologies in Welding and Materials Processing LTWMP (Odessa, 11–5 September, 2017)*, 73–77.
- Grabin, V.F. (1975) *Principles of physical metallurgy and heat treatment of welded joints of titanium alloys*. Kiev, Naukova Dumka, 263 [in Russian].
- Zamkov, V.N. (1986) *Metallurgy and technology of welding of titanium and its alloys*. Kiev, Naukova Dumka [in Russian].

Received 02.04.2020